Indian Journal of Engineering & Materials Sciences
Vol. 31, December 2024, pp. 799-811
DOI: 10.56042/ijems.v31i6.9562

Assessment of unmanned aerial system (UAS) based photogrammetric survey for road alignment using direct geo-referencing technology

Prakash Somani[a,b*], Amit Ranjan Chitranshi[c] , Arun Gaur[a], Amit Sain[a] & Ghanshyam Balotiya[a]

[a]Department of Civil Engineering, Malaviya National Institute of Technology Jaipur, Rajasthan 302 017, India
[b]Aayojan School of Architecture, Jaipur, Rajasthan 302 022, India
[c]National Highway Authority of India, New Delhi 110 075, India

Received: 13 March 2024; accepted: 31 October 2024

This study has compared the linear measurements of a road network using Differential Global Positioning System (DGPS)-based survey and UAS-based photogrammetric survey. To achieve this objective, 22 random Ground Control Points (GCPs) have been marked along the road network of 1.6 km length. The coordinates of the GCPs have been identified using DGPS and taken as base measurements. Coordinates of the GCPs have also been obtained through aerial images captured under various conditions, depending on Ground Sample Distance (GSD), overlapping of images, light conditions, shutter speed, and ISO of the sensor. The coordinate errors have been expressed as root mean square error (RMSE) relative to the base coordinates obtained through the DGPS and photogrammetric surveys. The results have demonstrated RMSE values as low as 0.263 mm, 0.305 mm, and 0.399 mm for the x, y, and z axes, respectively, under most test conditions, indicating sub-decimeter level accuracy. The selection of 22 random GCPs has been based on a stratified sampling approach to ensure comprehensive coverage and accuracy. It has been observed that the often-neglected camera settings can highly affect the location of the GCPs. Therefore, proper sensor settings must be considered while using UAS-based photogrammetric surveys.

Keywords: Accuracy evaluation, Georeferencing, Orthophoto, Photogrammetry, UAS

1 Introduction

As the world progresses, sectors requiring investment are demanding more focus and funding. Commerce, defense, production, and education sectors are proving to be the backbone of a country's development. These Sectors can or cannot be interrelated but all of these are affected by the transportation planning of that country. The growth of the highway sector is the benchmark of infrastructure development in developing nations. As highways are prominent for the transportation system, the big challenge is financing, management, and maintenance of highways[1]. Nowadays as the cost of construction and maintenance is on the higher side it is very important to use efficient and cost-effective alternatives for that purpose[2,3]. Accurate topographical information is essential for proper highway planning.

The earlier way for this topographical survey was a total station survey, which was time-consuming and has some constrained as it involves labor. Further, the Light Detection and Ranging (LiDAR) technique method comes out and started providing accurate data for road alignment applications[4]. Although the technique is effective up to a level but due to higher cost it does not fit in the efficient model. In this chain the Satellite imagery it was also used for accurate images and positioning but it is highly affected by weather conditions and problems in again reallocating the same point due to time taking of satellite to come into the same position[5].

The conventional methods in topographic and planimetric surveys under Highway Projects involve Total Stations to get positional coordinates of ground features and auto-level for the contours or vertical elevations. Typically, the surveys in the Road Projects are carried out through total stations to take x, y, z coordinates of the alignment to prepare a plan, profiles, and to identify nearby features like structures, electrical utility poles, trees, etc. through topographic surveys. Although, if done properly, road surveys carried out through traditional methods like total stations are advantageous in terms of inherent accuracies they carry, however, such surveys are time-consuming and laborious[6–8]. Such surveys are

*Corresponding author
(E-mail: prakashsomani197@gmail.com)

prone to human errors which have a cascading effect i.e., they increase with distance. The use of conventional methods poses serious challenges in inaccessible and inhospitable terrains. Such surveying methods sometimes expose the crew to vehicular traffic and unsafe conditions[9–12]. The use of UASs based photogrammetric survey has emerged as a new technological tool to carry out field works expeditiously and with desired accuracy levels. Utilizing an Unmanned Aerial System (UAS), a type of aircraft with no onboard crew or passengers and commonly known as a drone, allowing for fast, safe, and efficient engineering data collection, as well as allowing for 2D and 3D data visualization. Carrying out surveys through UASs is a time-effective method that has the potential to reduce/replace the laborious and cumbersome conventional traversing methods especially in green field Highway Projects and inaccessible terrains.

Rapidly growing technology increases the computing capacity with a reduction in the size of sensors at a lesser cost because this aerial survey can be done with small UASs. UAS system comes with multiple applications due to its ease of modification by the requirement[13]. The use of UASs in photogrammetric surveys of Highway Project is gaining importance due to inherent advantages like availability of actual site view, ease of surveys in inaccessible terrain, ease of gaining numerous information i.e., coordinates, offsets, etc. In a single field visit, ease of selection through multiple alignments and faster work with minimum manpower requirement. The high-resolution images obtained via a camera mounted on UASs are processed through photogrammetric techniques to obtain precise coordinates of the ground features which are further used to produce orthomaps and Digital Terrain Models for further Engineering use[2,6]. The UAS-based aerial surveys can be performed by any of these methods autonomously, semi-autonomously, or remotely controlled. Mainly UASs are classified as three types (Fixed Wing, Single Motor & Multi-Motor) each having individual pros and cons and select as per requirement.

The use of Unmanned Aerial Systems (UAS) in infrastructure and land use planning has advanced significantly, integrating technologies such as deep learning, machine learning, and high-resolution sensors.Wang et al.[14]utilized UAS imagery combined with deep learning and machine learning to identify the utilization status of rural courtyards in North China, achieving high precision and cost-effectiveness for large-scale surveys. Chen et al.[15]developed a UAS-based system for pothole detection, offering a low-cost alternative to traditional methods with high accuracy in depth and volume evaluation. Li *et al*.[16] focused on bridge damage detection using data fusion of UAS, LiDAR, and imagery, achieving precise damage assessment essential for infrastructure maintenance. Nomqupu *et al*.[17] enhanced pothole detection by integrating a sigmoid calibration function into entropy thre sholding segmentation on UAS multispectral imagery, improving recognition accuracy. Wang and Huang[18]proposed a method for manhole cover classification using UAS imagery and super-resolution reconstruction, significantly reducing survey time and labor costs. Xue *et al*.[19] introduced MAD-UNet, a network for rural building extraction from UAS images, achieving high accuracy and minimizing misclassifications. Egodawela *et al*.[20] presented a deep learning approach for surface crack detection in UAS-assisted infrastructure inspections, demonstrating high accuracy and segmentation performance. Soon *et al*.[21]examined the challenges of UAS implementation in Malaysian infrastructure projects, proposing a framework to promote adoption and address regulatory and industry barriers. García-Fernández *et al*.[22]improved real-time processing for UAS-mounted Ground Penetrating Radar systems, enabling effective detection of subsurface targets. Cui *et al*.[23]explored integrating UAS with public transit for delivery, highlighting benefits such as increased revenue, reduced emissions, and congestion mitigation.

The integration of UAV technology in road alignment surveys is gaining momentum due to its efficiency, accuracy, and cost-effectiveness. Fig. 1 illustrates the co-occurrence of key terms associated with UAV surveys for road alignment, as extracted from the Scopus database. This network graph underscores the interconnectedness of various disciplines and technologies involved in UAV applications. This co-occurrence network reinforces the multidisciplinary approach required for optimizing UAV technology in infrastructure projects, emphasizing the need for integrated systems that leverage various technologies and methodologies. The adoption of UAVs, coupled with advanced data processing techniques, promises significant improvements in the efficiency and accuracy of road alignment surveys, thereby contributing to more effective infrastructure management and planning.

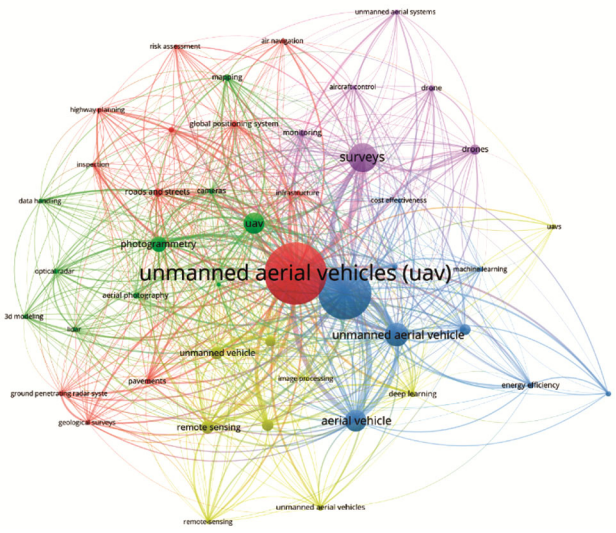

Fig. 1 — Co-occurrence network graph of terms related to UAV survey for road alignment.

While previous studies have leveraged UAV technology for infrastructure assessment, our approach introduces several groundbreaking advancements that address the limitations of traditional methods. Traditional road alignment surveys often rely on labor-intensive, costly ground surveys and are limited by the scope and efficiency of data collection methods[14]. Our study, however, integrates advanced deep learning and machine learning algorithms with high-resolution UAV imagery, offering a comprehensive and scalable solution for road alignment and infrastructure monitoring. Unlike the focused applications in pothole detection[15] and bridge damage assessment[16], our method employs a diverse array of algorithms to evaluate multiple infrastructure aspects simultaneously. This not only enhances the accuracy of defect detection but also significantly reduces the time and cost associated with large-scale surveys. Additionally, our approach facilitates real-time data processing and immediate application in field conditions, setting a new standard for efficiency and effectiveness in UAV-based infrastructure assessments[14,17]. By addressing the critical needs for scalability, cost-effectiveness, and accuracy, our study represents a significant advancement in the application of UAV technology for modern infrastructure management and planning.

1.1 Scenario in India

In recent years the use of UAS based photogrammetric surveys is gaining importance in Road construction projects of India. However, it is observed that the consultants engaged in UAS based photogrammetric surveying are carrying out the aerial survey and photogrammetric processing works in absence of any standards, guidelines, or specifications on this subject. The Indian Road Congress is yet to issue any standard/specifications/guidelines regarding UAS based photogrammetric survey of Highway Projects. Although Government Agencies like Indian Railways and National Highway Authority of India (NHAI) are utilizing this technology in some of their survey works, however, the specifications and methodologies remain non-standard, uncertain, and un-researched[24].

The above uncertainties are liable to bring sub-standard products and practices in the industry creating further confusion over the use of this technology. An explicit document having comprehensive details of UAS-based photogrammetric survey their use in Highway Projects is yet to be prepared so that the technology can have a common platform and can be easily adopted by various stakeholders of the Highway Industry.

1.2 Direct Geo-Referencing technology

The existing photogrammetric surveys with UASs are being carried out with the use of multiple ground control points per km thus again making the whole process time taking and prone to manual error while setting of ground control points along the alignment. Direct Geo-Referencing Technology has the potential to directly geotag the aerial images and eliminates the requirement of ground control points by 90%[25]. Such an attempt has been made to find out the appropriateness of UAS-based photogrammetric surveys using direct geo-referencing technology in Road/Highway Projects in opposition to accuracy requirement under various accuracy standards. This study mainly focused on identifying the best flight planning parameters, camera settings, resolution requirements, and daylight conditions required to achieve the best out of this technology.

2 Material and Methods

2.1 Study area

The study is performed at the main arterial road of an institute campus starting from entrance gate and goes to hostel building as shown Fig. 2. The road measures 1.66km on the ground and 1.54km aerially, aerial distance is lesser due to curvilinear path require a greater number of GCP. The open field behind the badminton court was selected as the take-off &

Fig. 2 — Study area showing the main arterial road of the institute campus, from the entrance gate to the hostel building.

Fig. 3 — Distribution of reference GCP, ground control points (GCP) and checkpoints along the study area.

Table 1 — Coordinates of selected points by Differential Global Positioning System (DGPS).

Point	X (m)	Y (m)	Z (m)	Point	X (m)	Y (m)	Z (m)
3	580273.031	2971765.334	370.691	TS13	580820.221	2971612.105	373.778
4	580259.675	2971723.270	369.721	TS14	580909.035	2971609.197	374.386
TS1	580321.811	2971765.138	370.872	TS18	580999.096	2971562.645	373.342
TS2	580339.283	2971708.319	370.469	TS21	581082.328	2971563.977	373.761
TS3	580390.748	2971754.799	371.55	TS22	581138.665	2971458.662	370.391
TS5	580488.181	2971746.372	372.035	TS23	581202.872	2971470.603	370.546
TS 6	580481.853	2971625.185	383.576	TS24	581203.860	2971500.527	372.066
TS8	580564.726	2971679.917	371.825	TS25	581285.314	2971453.602	370.952
TS9	580594.541	2971630.668	371.601	TS26	581376.689	2971420.070	369.511
TS10	580696.498	2971603.832	371.945	TS27	581455.921	2971341.569	368.548
TS11	580689.296	2971654.904	372.679	TS29	581524.255	2971416.688	370.759

landing point. The internal roads and other landscapes, buildings, etc. of the campus are a prototype of actual field conditions. To achieve the above objective, a total of around 22 GCPs were established as mentioned in Fig. 3 and coordinates were recorded using DGPS systems (in fast static mode) with 2cm accuracy. Coordinates of selected by DGPS are shown in Table 1.

2.2 UAS specification

The UAS used in the experiment is a High Winger V Tail fixed-winged drone, indigenously manufactured by AUS Pvt Ltd, Bangalore, as shown in Fig. 4. The UAS has a wingspan of1800mm wingspan and 1100mm in length. The UAS is equipped with all basic instrumentations namely- Autopilot, Survey grade Post processing kinematics (PPK) or Real time kinematics

Fig. 4 — High winger V tail fixed-winged UAS used in the study.

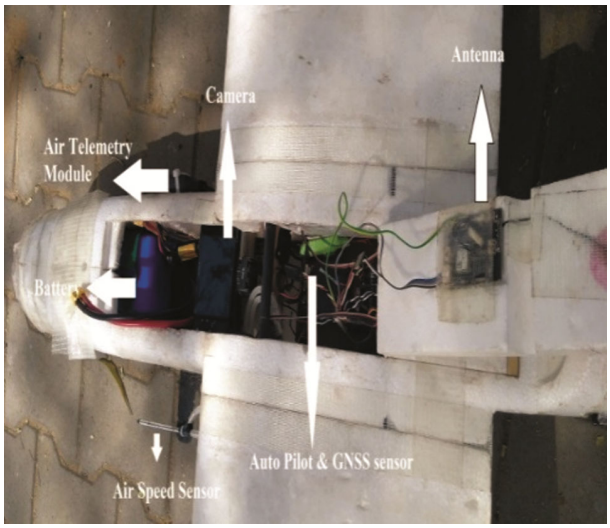

Fig. 5 — Sensor used inside the UAS2.3 collection of data.

(RTK) supporting Global Navigation Satellite System (GNSS) sensor, dual-frequency antenna, airspeed sensor, air telemetry module, and push-type propeller at the endure mentioned in Fig. 5. The UAS has a ground speed of 15m/s. The power requires for this equipment is supplied by a rechargeable battery of 6000mAh capacity. The total weight of the UAS including all equipment was 3kg. As payload, Sony DSC RX100 M2 camera was mounted on UAS in an enclosure such that the x-axis of the camera is perpendicular to the flight line. In this camera Exmor R™ CMOS sensor of 1 inch (13.2 mm wide and 8.8 mm height) sized was in build. The camera can capture images of 20Megapixels with ISO sensitivity of 100-25600 and shutter speed at 30 sec to 1/2000 sec. Skylink developed by AUS Pvt Ltd was used as flight planning software. Open-sourced RTKLib was used for PPK processing of image coordinate logs obtained from the onboard GNS Ssensor. Commercial software Pix4D was used for photogrammetric processing of images to obtain orthomaps, Digital surface model (DSM) and Digital terrain model (DTM).

A UAS-based photogrammetric survey is done in the following steps planning, data collection, data processing, and analyzing. After the selection site for the survey firstly flight planning is prepared then groundwork is done. Planning involved site selection on Google earth interface and creation of KML file with an approximate location of the GCPs/CPs as shown in Fig. 6. A centerline was marked along the stretch and an area within 100m each side of the centerline was marked as a buffer area. The flight plan was created on Skylink softwares[26] for each flight (experiment) with the formation of grids out of parameters like GSD, Overlap, and Grid angle. For each flight, different flight plans were created. The groundwork included marking of distinctive squares of size 2feetx2feet on the ground at the approximate locations of GCPs/CPs marked in the KML file. It was ensured that the marking was done at locations that could be visible from an aerial UAS without any obstruction of trees, cables, etc. Subsequently, the coordinates of the center of these square markings were taken with the help of 2 Nos Trimble R4 DGPS receivers. A base DGPS receiver in static mode was set on the roof of the Prabha Bhawan Building. The second DGPS receiver was used to take 30 minutes static readings at other GCPs/CPs keeping the base receiver on till readings on all GCPs/CPs were completed. The coordinates were further refined by post-processing corrections in Trimble software. The positional coordinates were taken in the Universal Transverse Mercator (UTM) system with World Geodetic System 1984 (WGS84) datum and Earth Gravitational Model(EGM96) altitude.

Before the start of flying, a GNSS senor was set as a base at the same point on top of the building where the base station was set. With the base sensor on throughout the flight, the onboard GNSS sensor (rover) on UAS geo-tags each photograph which was saved in the onboard memory card. The camera was set to a fixed focal length of 13.4mm with a field of view of approximately 94 degrees. Before each flight, the camera parameter (ISO, Shutter speed) was set on the camera and the GSD-overlap setting was done on the Skylink software. The UAS was launched by hand

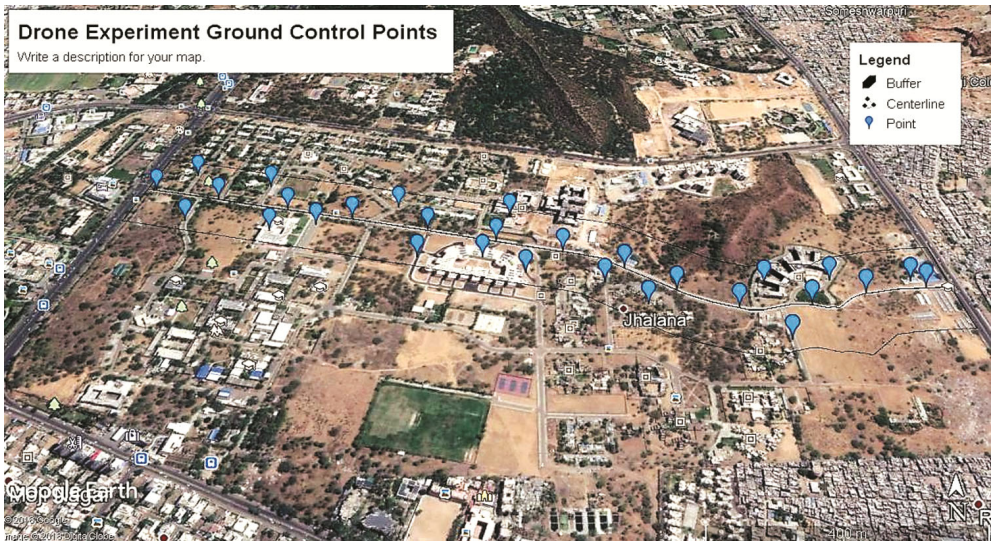

Fig. 6 — Google earth interface showing the marked points, buffer line, and centerline of the study area.

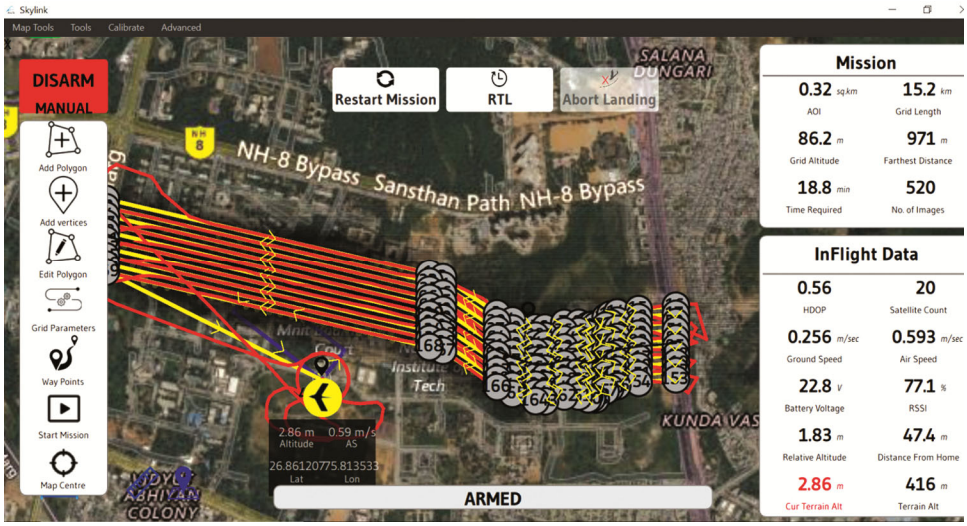

Fig. 7 — Sky-link monitor screen displaying the flight pattern and flight details during the UAS operation.

with manual control and once it achieved an altitude of 60m, the autopilot took over the control through Skylink software. The UAS was again controlled manually once the landing mode was initiated. After maneuvering on the grid pattern pre-defined for the experiment, the UAS returned to the same location with a belly landing.

The real-time flight status and quality of the UAS along the pre-defined grid were monitored on the Skylink running in the ground station laptop as shown in Fig. 7. The laptop was connected with the UAS through radio frequency with the ground telemetry module on a laptop and aerial telemetry module on the UAS. After each experiment, the aerial images were copied from the camera memory on a laptop. The geo-tags of each image which were recorded on a separate memory card were also copied onto the laptop. It was ensured that a separate folder is created for each experiment in which its images and geo-tags were saved. During the experiment, it was seen that the average ground speed of the UAS when flying from main gate towards hostel was 12-13m/s and when the UAS returned and fly back towards main gate, the ground speed was about 18-20m/s. The Autopilot checked the ground speed when it crossed 20m/s. The autopilot also regulated the camera trigger speed with the speed of the UAS such that the desired overlap of images is achieved.

Data collected by individual flights are processed with image processing software. First, the image

Table 2 — Details of UAS flight parameters, including GSD, side overlap, ISO, shutter speed, flight time, and method used UAS

Flight	GSD (cm/pixel)	Side Overlap (%)	ISO	Shutter Speed (sec)	Flight Time	Method
A	2	80	100	1/1600	11.00am	PPK
B	3	80	100	1/1600	12.05pm	PPK
C	4	80	100	1/1600	11.00am	PPK
D	5	80	100	1/1600	12.45pm	PPK
E	3	60	100	1/1600	12.30pm	PPK
F	3	70	100	1/1600	1:00pm	PPK
G	3	80	100	1/1600	10.00am	PPK
H	3	80	200	1/1600	10.00am	PPK
I	3	80	400	1/1600	10.30am	PPK
J	3	80	100	1/640	1.00pm	PPK
K	3	80	100	1/1000	1.30pm	PPK
L	3	80	100	1/1600	3.00pm	PPK
M	2	80	100	1/1600	11.00am	GCP
N	3	80	100	1/1600	10.00am	GCP

Table 3 — Height of UAS above ground level, flight durations and number of images taken at different GSD.

Ground Sample Distance (GSD)	AGL (m)	Number of Images	Flight Duration (min)
2	90	520	18.8
3	135	343	14.5
4	172	184	10.9
5	220	101	8.09

coordinates were corrected in the PPK processing with the base coordinates. For each experiment, the images along with the (corrected) geo-location file were uploaded as input files in the image processing software Pix4D[27]. In output coordinates of selected points, area, volume, DSM, DTM, and Orthomosaic map are obtained. The quality report generated in the processing gave the difference between the checkpoint's coordinates obtained from image processing to the coordinates obtained from DGPS. These errors can further be analyzed by different standards for mapping.

In this study, fourteen flights are planned by varying parameters like GSD, Overlapping, ISO, shutter speed, and sunlight. To inspect the accuracy of the PPK method over the GCP method two flights at different GSD are done. The coordinates of the checkpoints obtained after photogrammetric processing of images sets of each experiment were compared with the respective coordinates obtained through DGPS. Flight details with all parameters are mentioned in Table 2.

Ground sample distance is directly proportional to the height of flight from ground level and also affects the flight duration and number of images required or processing. Table 3 shows the Above ground level (AGL), number of images, and flight time for corresponding GSD at 80% overlapping. Figure 8 and 9

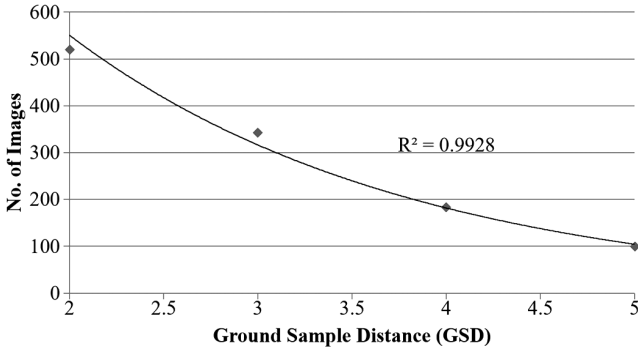

Fig. 8 — Relationship between the number of images taken and the ground sample distance (GSD).

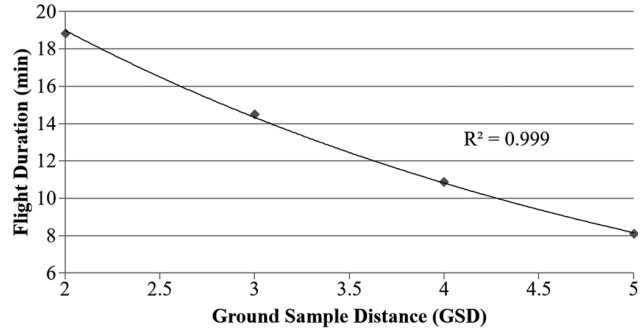

Fig. 9 — Relationship between the flight duration and the ground sample distance (GSD).

demonstrates as altitude AGL or GSD increases, flight duration, and the number of images taken decrease because each image covers more area, and, therefore, fewer laps and images are needed. This occurs independently of the forward and side overlap settings, although higher percentages increase flight time and the number of images taken[20].

The 22 random GCPs were strategically placed using a stratified random sampling technique to

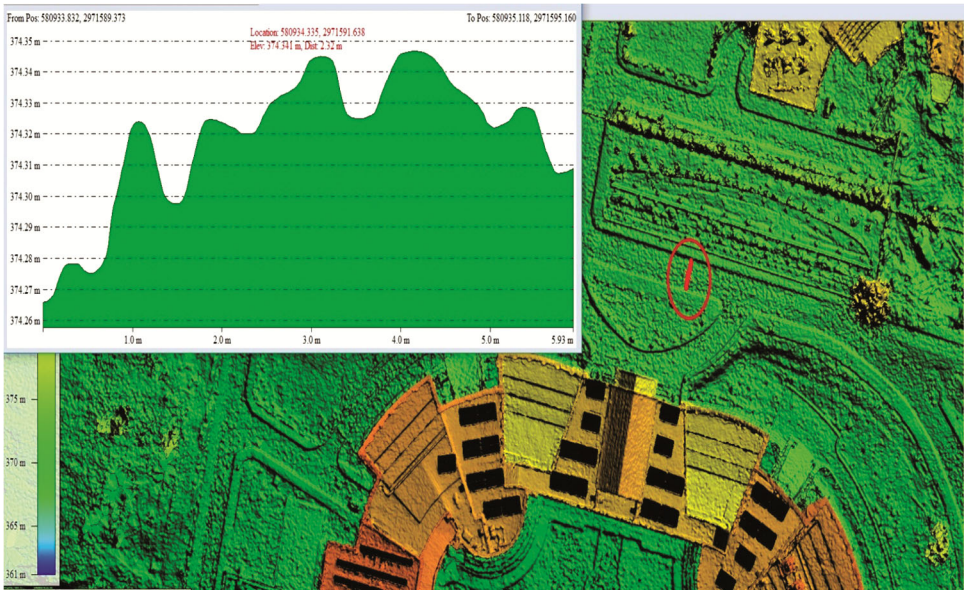

Fig. 10 — Digital Surface Model (DSM) of the selected section, providing cross-sectional details of the alignment.

Table 4 — RMSE values (meter) for all direction (X, Y, Z) of different flight.

Flight	A	B	C	D	E	F	G	H	I	J	K	L	M	N
RMSE X	0.124	0.073	0.095	0.057	0.102	0.084	0.116	0.045	0.050	0.056	0.064	0.066	0.168	0.123
RMSE Y	0.096	0.090	0.157	0.126	0.083	0.122	0.111	0.099	0.108	0.088	0.109	0.100	0.472	0.435
RMSE R	0.157	0.116	0.184	0.138	0.132	0.148	0.161	0.109	0.119	0.104	0.126	0.120	0.501	0.452
RMSE Z	0.094	0.095	0.083	0.102	0.123	0.071	0.062	0.086	0.063	0.077	0.288	0.091	5.678	4.916

ensure comprehensive coverage and accurate georeferencing. This method allowed us to capture the variability in terrain and infrastructure features, ensuring that all significant areas were represented. GCP locations were chosen to avoid obstructions and maintain line-of-sight with the UAV. The High Winger V Tail fixed-winged drone equipped with a Sony DSC RX100 M2 camera was selected for its high-resolution imaging capabilities. Camera settings, including a 13.4mm focal length, ISO sensitivity between 100 and 25600, and a shutter speed of 1/1600 seconds, were optimized to ensure image clarity and efficient data collection. The Ground Sample Distance (GSD) was set to 3cm, balancing resolution and processing time, based on best practices and preliminary test flights. These choices ensured the accuracy and reliability of our data for the study.

2.4 Digital surface model and orthomap

Digital Surface Model (DSM) provide cross sectional details of contour interval 0.5m or more and ortho map generated from the photogrammetric processing of the image show clear and measurable details of the alignment including the planimetric features, trees, structures, gardens of the campus. The DSM gives the cross-sectional details of the alignment with a contour interval of any value greater than the GSD. DSM accuracy is directly affected by number of GCPs establishment. The profile extracted from the cross-sectional details can be used to mark the centerline of the highway. The profile of road section obtained from DSM generated and shown in Fig 10.

3 Results and Discussion

The accuracy achieved through photogrammetric surveys should meet the standards for such scales. The National Standard for Spatial Data Accuracy(NSSDA), Federal Geographic Data Committee, US and American Society for Photogrammetry and Remote Sensing (ASPRS)[21] Positional Accuracy Standards for Digital Geospatial Data are considered for validation of the data set collected in this study. The NSSDA and ASPRS both asses positional accuracy based on root-mean-square error (RMSE). RMSE values for data set of all flight by DGPS reading are calculated in x, y, and z-direction are mentioned in Table 4 RMSE in a radial direction is calculated for horizontal accuracy assessment, whereas z-axis RMSE is used for vertical accuracy.

Table 5 — ASPRS standard accuracy values for horizontal and vertical accuracy classes.

Accuracy Class	RMS Exor RMSEy(cm)	RMSEr(cm)	Horizontal Accuracyat 95% Confidence Level (cm)	RMSEz	Vertical Accuracy (at 95%Confidence Level (cm)
I	2.5	3.5	6.1	1.0	2.0
II	5.0	7.1	12.2	2.5	4.9
III	7.5	10.6	18.4	5.0	9.8

Table 6 — NSSDA standard accuracy values for different flights.

Flight	A	B	C	D	E	F	G	H	I	J	K	L	M	N
Horizontal	0.27	0.2	0.31	0.22	0.23	0.25	0.28	0.18	0.19	0.18	0.21	0.2	0.78	0.7
Vertical	0.18	0.19	0.16	0.2	0.24	0.14	0.12	0.17	0.12	0.15	0.56	0.18	11.13	9.6

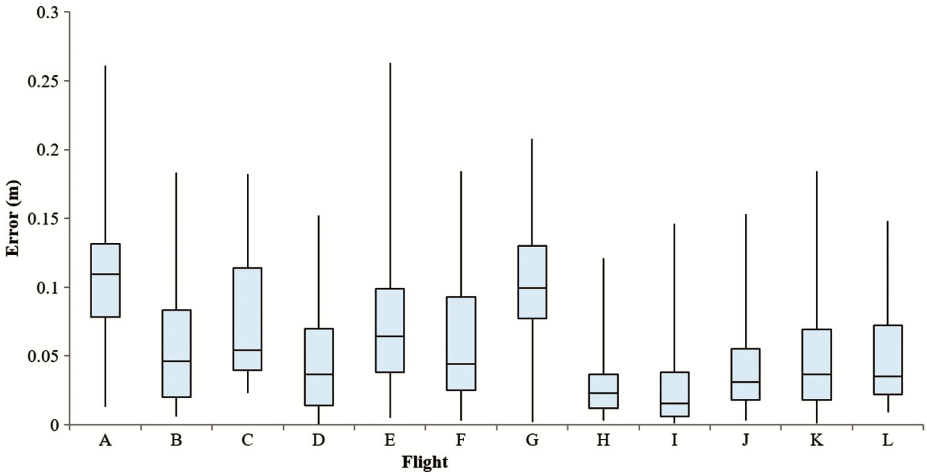

Fig. 11 — X-Axis errors for all flight experiments, showing the variation in accuracy.

3.1 ASPRS accuracy

The ASPRS horizontal accuracy standard is based on accuracy classes using root mean square error statistics, whereas the ASPRS vertical accuracy standard is based on accuracy classes using RMSE statistics in non-vegetated terrain, and 95th percentile statistics in vegetated terrain[21]. The scale of the map is also required to estimate the accuracy class. All highway maps are plotted of 1:200 scale, therefore 1:200 map scale accuracy is chosen for validation. ASPRS horizontal and vertical accuracy are shown in Table 5.

3.2 NSSDA Accuracy

The NSSDA assumes that systematic errors have been eliminated as best as possible. If both horizontal and vertical errors are normally distributed, then factor 2.4477 and 1.9600 are used to evaluate horizontal and vertical accuracy at a 95% confidence level[22]. NSSDA horizontal and vertical accuracy are shown in Table 6.

$$\text{Horizontal Accuracy} = 2.4477 \times \text{RMSEr} = 2.4477 \times \sqrt{\text{RMSEx}^2 + \text{RMSEy}^2} \quad ...(1)$$

$$\text{Vertical Accuracy} = 1.9600 \times \text{RMSEz} \quad ...(2)$$

3.3 Comparative statement

Accuracy assessments for all flight data set in x, y, and z-axis are done by both NSSDA and ASPRS methods. In x-axis flight, E's single point error doesn't meet with standards, whereas in y-axis flight D, F, H, I, J, L, and M's multiple point errors don't fulfill the corresponding standard values. Flight A, C, D, E, G, H, I, J, L, and N's multiple point errors in the z-axis are not in range of standards. Fluctuations of error for different flights in x, y, and z-axis are graphically represented in Fig. 11, Fig. 12 and Fig. 13. It can be observed that maximum errors in x, y, and z-axis are respectively 0.263, 0.305, and 0.399 mm by the PPK method. The correlation coefficient for all data sets of PPK methods flight is about 0.9999 which means values observed by the PPK method are nearly the same as DGPs readings. For validating the values obtain by the PPK method, a t-test was performed on all data sets and observed there is no significant difference between the means of PPK method values and DGPS reading.

RMSE values obtained using the GCP method are greater compared to the PPK method, considering 2-GSD and 3-GSD. The results of the GCP method

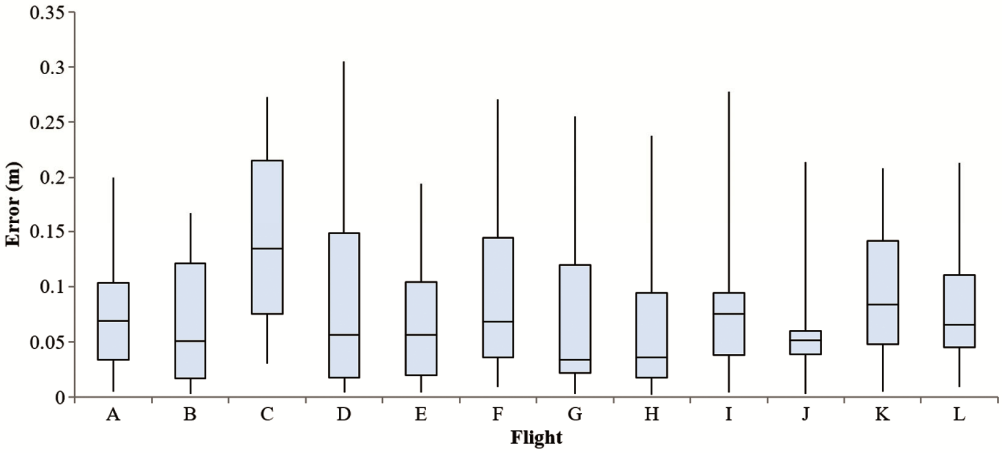

Fig. 12 — Y-axis errors for all flight experiments, illustrating the positional accuracy.

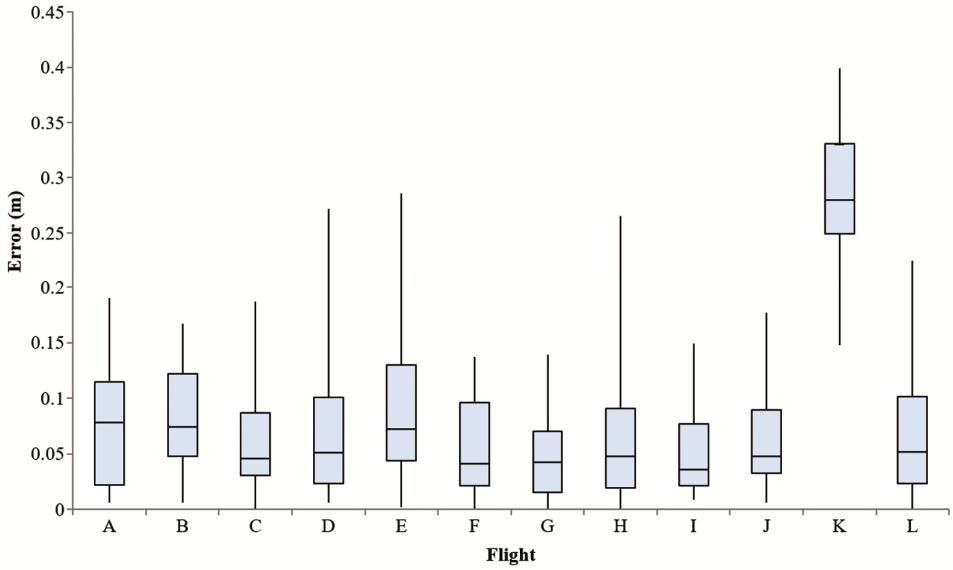

Fig. 13 — Z-axis errors for all flight experiments, demonstrating the vertical accuracy.

represented in Fig. 14, shows high RMSE z values touching 5 meters whereas RMSEx and RMSEz are also substantially higher as compared to the direct geo-reference method results. We can infer that more than 3 GCPs are required for a linear stretch of 1.6km to get same level of accuracies comparable to PPK processed photogrammetric outputs. This validates the use of Direct Geo-reference PPK technology in photogrammetric surveys of linear stretches.

RMSE values obtain by different flight varying parameters like GSD, Overlapping, ISO, shutter speed, and sunlight are compared in Fig. 15-19 to find out a suitable setting for UAS.

It can be analyzed from Fig. 15 RSME z values have an increasing trend with the GSD. RSME x and y values are minimum for 3 cm GSD.Based on the results, it can be inferred that a 3cm-4cm GSD is suitable for the topographical survey of the Road/Highway Project and can give the RMSE values within the sub-decimeter level. As the increase in time of flight would increase the number of flights for a particular project, the larger number of images would further mean more processing time. The calculation time will increase exponentially (cubically) with the total number of pixels in a map[23]. This means that the grid resolution needs to match the capabilities of our computer and the time given to complete a GIS project[24]. The processing time for each experiment on Pix4D software was around 4 hours for a 3cm GSD. Hence a judicious decision is required to be taken on

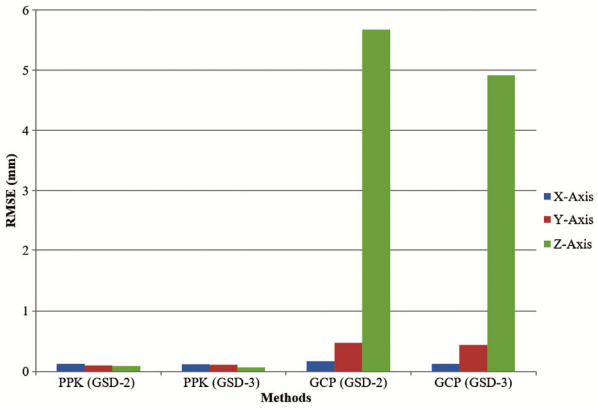

Fig. 14 — Comparison of RMSE values obtained using the ground control points (GCP) method and the post-processing kinematics (PPK) method.

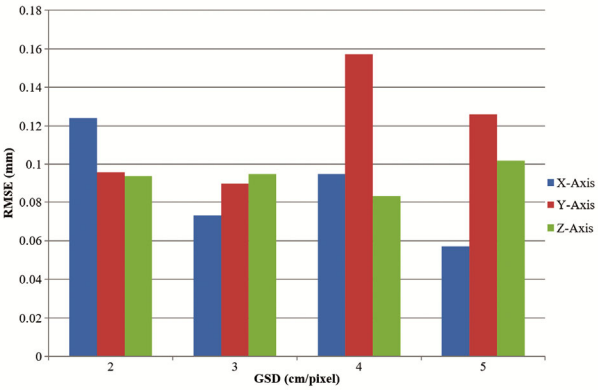

Fig. 15 — RMSE values at different ground sample distances (GSD), highlighting the impact on accuracy.

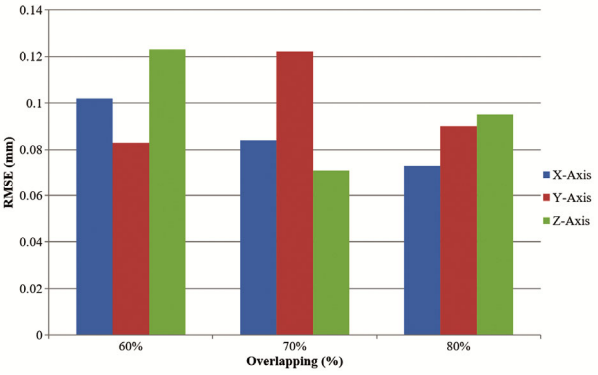

Fig. 16 — RMSE values at different overlapping percentages, showing the effect on accuracy.

the selection of GSD such that it meets both accuracy and detailing requirements.

The results are shown in Fig. 16 foran increase in side overlap there is a substantial decrease in RMSEx and RMSEz values. As discussed, an overlap of images does feature matching between two images which is required for the creation of 3D geometry of a scene through photogrammetric processing. Although an increase in overlaps increases the matching features and resultant point cloud density[25], at the same time it increases the flight time and the number of images thus decreasing the efficiency of the process. Hence an optimum overlap is required to be adopted to ensure that the RMSE values are within an acceptable range and at the same time the process is time-efficient. Overlap also depends on the type of image processing software being used like image processing company Pix4D recommends 75 % frontal and 60 % side overlap in general cases while Agisoft recommends 80 % forward overlap and 60 % side overlap. It should be ensured that the camera shutter speed should be faster than the camera trigger pulse in case of higher frontal overlap (80%-90%). From the results, it is observed that an overlap of 80% gives reasonably good RMSE values (~10cm) with 3cm GCP and may be adopted for highway projects.

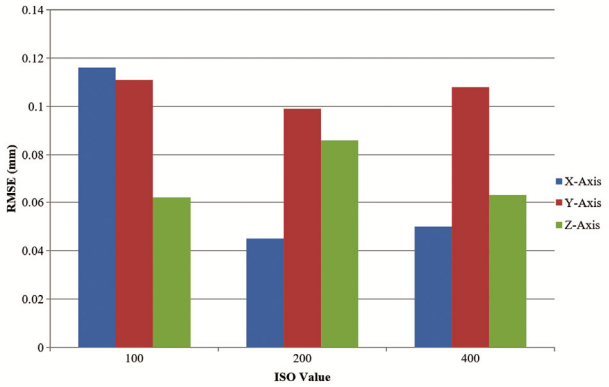

Fig. 17 — RMSE values at different ISO settings, illustrating the influence of camera sensitivity on accuracy.

The results obtained by changing camera ISO settings show encouraging results represented in Fig. 17. The results show that RMSEx and RMSEy decrease with an increase in ISO from 100 to 200 or from 100 to 400. The RMSEz is almost similar for ISO100 and ISO400; however, it increases slightly with ISO200. The camera ISO defines the sensitivity of the sensor towards the light[26]. The lower the ISO, the less sensitive it is towards the light. Higher ISO means more sensitive to light and hence it is used in dim light[27]. The result shows that ISO200 and ISO400 gives lower RMSE values than ISO100 which was the default ISO in all other experiments. Hence it can be inferred that camera ISO also plays an important role in photogrammetric accuracy of features and judicious selection of ISO should be done depending upon the daylight.

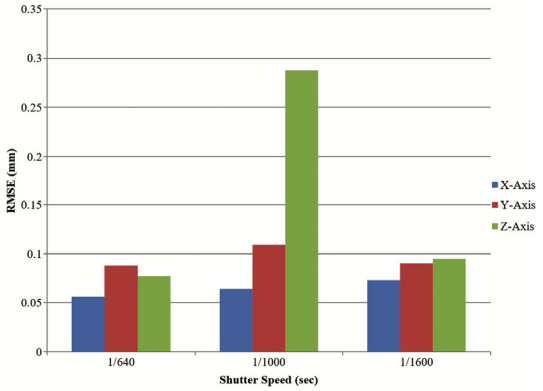

Fig. 18 — RMSE values at different shutter speeds, showing the impact on photogrammetric accuracy.

The camera shutter speed experiments show interesting trends as shown in Fig. 18. The experiments were conducted at three shutter speed 1/640, 1/1000, and the default setting of 1/1600. The RMSEx as well as RMSEy values show improvement with a decrease in shutter speed. However, the RMSEz values show abrupt peak (~28cm) at shutter speed 1/1000s while having reasonably lower values at shutter speed 1/1600(~9cm) and 1/640(~7cm).

As a standard practice, aerial photography shall not be undertaken when the angle of sun rays is less than thirty (30) degrees above the horizon[6,7,26]. The results shown in Fig 19 there are slight deterioration in RMSE values in the experiment conducted at 10am (~11cm) as compared to the experiment conducted at 3pm (~9cm) with all parameters identical. This could be due to the requirement for different camera ISO settings as there were changes in lighting conditions. The increase in ISO drastically decreased the RMSE values. Hence it can be inferred that the ideal time for UAS based photogrammetric survey is between 10am to 3pm when the angle of sun rays is more than thirty (30) degrees above the horizon. However, the ISO settings should be judiciously selected based on the lighting conditions.

The ISO and shutter speed experiments show that the photogrammetric accuracies are highly affected by camera settings like ISO and shutter speed which controls the amount of light on the sensor. The best RMSE values observed in various experiments under this work pertains to changes in camera settings like ISO and shutter speed. Images obtained with ideal camera settings concerning UAS height AGL and overlaps are sharper and focused which in turn will have better feature matching and hence better photogrammetric output/accuracy.

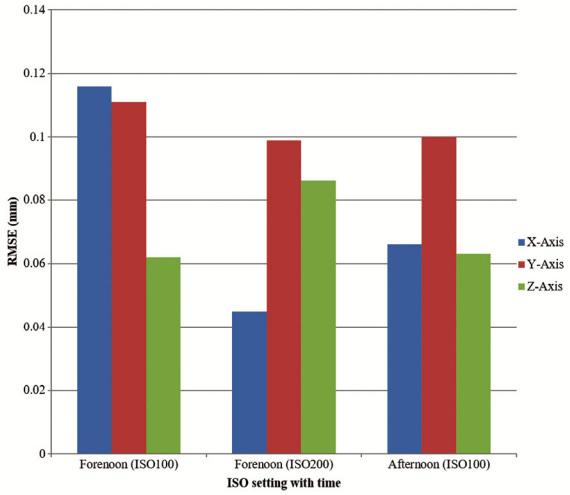

Fig. 19 — RMSE values at different times of the day, demonstrating the effect of sunlight on accuracy.

The primary objective of this study was to evaluate the accuracy and feasibility of using UAV-based photogrammetric surveys for road alignment and infrastructure monitoring. Our first research question focused on assessing the effectiveness of different flight parameters and GCP configurations in achieving high photogrammetric accuracy. The results showed that the PPK method provided significantly better accuracy compared to the GCP method, with RMSE values in x, y, and z axes being within sub-decimeter levels. The second research question addressed the impact of various UAV flight parameters, such as GSD, overlap, ISO, and shutter speed, on photogrammetric accuracy. Our experiments revealed that a GSD of 3cm to 4cm provided optimal accuracy, with RMSE values within acceptable ranges. Additionally, increasing the image overlap to 80% significantly improved RMSE values, highlighting the importance of overlap in ensuring accurate 3D geometry creation. Furthermore, the experiments on ISO and shutter speed demonstrated that these camera settings play a crucial role in photogrammetric accuracy. Higher ISO values (200 and 400) resulted in lower RMSE values compared to the default ISO 100, while a shutter speed of 1/640s provided the best balance between x, y, and z-axis accuracy. Our third research question explored the application of UAV surveys in various lighting conditions. The results indicated that conducting surveys when the sun is at least 30 degrees above the horizon (between 10 am and 3 pm) yields better accuracy due to optimal lighting conditions. This insight is crucial for planning UAV surveys to ensure consistent and high-quality data capture.

The study's findings provide strong evidence that UAV-based photogrammetric surveys, when optimized for flight parameters and camera settings, can offer highly accurate and efficient solutions for road alignment and infrastructure monitoring. These results not only validate our research hypotheses but also offer practical recommendations for practitioners in the field, enhancing the applicability and reliability of UAV technology in infrastructure projects.

4 Conclusion

The project has demonstrated that UAS-based photogrammetric surveys have tremendous potential in preparing cost and time-effective Linear Project Reports, which otherwise take long durations and often disrupt project timelines UAS. The sub-decimeter level achievable RMSE's prove that the technology is highly effective in reducing the time and human error in various surveys associated with Highway Projects.

The sub-decimeter accuracies in x, y, and z obtained in most experiments validate the potential of direct geo-referencing technology, which significantly reduces the need for multiple GCPs. The conventional method requires setting up of minimum 5-8 GCPs per km which itself is a costly, cumbersome, time-consuming, and error-prone activity. The highly erroneous results obtained while processing images of two experiments using 3 GCPs shows that much more than 3 GCPs are required to achieve direct geo-referencing level results even for a 1.6km stretch.

The parameters which gave the best results under the direct geo-referencing method are 3cm GSD, 80Sx70F overlap, 200ISO, 1/1600 shutter speed, and time 10am. The RMSEx, RMSEy, and RMSEz values obtained in the experiment with the above parameters are 4.5cm, 9.9cm, and 8.6cm respectively. Table-4 shows that these RMSE values meet almost all the Indian and International map accuracy standards. The slight aberration in y values has been observed in the results which may be due to lack of Inertial Navigation Sensor (INS) in the UAS which measures the yaw, pitch, and roll during the flight which further refines the coordinates of the images. The survey-grade GNSS-INS sensors are quite costly as compared to the GNSS sensors which were used in the UAS.

The UAS based photogrammetric surveys have the potential to replace conventional methods for surveys of linear projects except for areas dense forest canopies, standing crops, water bodies, etc. where the light cannot penetrate. However, UASs are no substitute for field visits which are required for soil investigation, an inspection of facilities not visible from UAS imagery like the underside of culverts, bridges, underground utilities, etc.

References

1 Agüera-Vega F, Carvajal-Ramírez F & Martínez-Carricondo P, *Meas*, 98 (2017) 221.
2 Outay F, Mengash H A & Adnan M, *Trans Res A Policy Prac*, 141(2020) 116.
3 Hugenholtz C H, Whitehead K, Brown O W, Barchyn T E, Moorman B J, LeClair, A & Hamilton T, *Geomorphology*, 194 (2013)16.
4 Ajayi O G, Palmer M & Salubi A A, *Remote Sens Appl: Soc Environ*, 11(2018) 220.
5 Le Mauff B, Juigner M, Ba A, Robin M, Launeau P & Fattal P, *Geomorphology*, 304 (2018) 121.
6 Eltner A, Baumgart P, Maas H G & Faust D, *Earth Surf Process Landf*, 40(2015) 741.
7 Gabrlik P, *IFAC-Papers OnLine*, 48 (2015) 380.
8 Salvo G, Caruso L, Scordo A, Guido G, & Vitale A, *Eur J Remote Sens*, 50 (2017) 343.
9 Wang D & Huang Y, *Appl Sci*, 14 (2024) 2769.
10 Chen S, Laefer D F, Zeng X, Truong-Hong L & Mangina E, *J Surv Eng*, 150 (2024) 05024001.
11 Li H, Chen Y, Liu J, Che C, Meng Z & Zhu H, *Comput-Aid Civil Infrastruc Eng*, 39 (2024) 1197.
12 Nomqupu S, Sali A, Nyamugama A & Ndou N, *Appl Sci*, 14 (2024) 2670.
13 Wang M, Xu W, Cao G & Liu T, *Build Simul*, 17 (2024) 799.
14 Xue H, Liu K, Wang Y, Chen Y, Huang C, Wang P & Li L, *Sensors*, 24 (2024) 2393.
15 Egodawela S, Gostar A K, Buddika H S, Dammika A J, Harischandra N, Navaratnam S & Mahmoodian M, *Sensors*, 24 (2024) 1936.
16 Soon T K, Teng N C, Wei N T, Tiong C C, Mukhlas N A & Shah M S A, *ASEAN Eng J*, 14 (2024) 237.
17 García-Fernández M, Álvarez-Narciandi G, Laviada J, López Y Á & Las-Heras F, *ISPRS J Photogram Remote Sens*, 212 (2024) 1.
18 Cui S, Yang Y, Gao K, Cui H, & Najafi A, *Trans Res A Policy Prac*, *183* (2024) 104048.
19 Barry P & Coakley R, *Int Arch Photogramm Remote Sens*, 2 (2013) 2731.
20 Haala N, Cramer M, & Rothermel M, *Int Archives Photogramm, Remote Sens and Spatial Inform Sci*, 40 (2013) 183.
21 American Society for Photogrammetry and Remote Sensing (ASPRS), *Photogramm Eng Remote Sens*, 81 (2015) A1-A26.
22 López F J & Gordo A D, *J Surv Eng*, 134 (2008) 39.
23 Colomina I & Molina P, *ISPRS J Photogramm Remote Sens*, 92(2014) 79.
24 Hengl T, *Comput Geosci*, 32 (2006) 1283.
25 Dandois J P, Olano M & Ellis E C, *Remote Sens*, 7 (2015) 13895.
26 Mancini F, Dubbini M, Gattelli M, Stecchi F, Fabbri S & Gabbianelli G, *Remote Sens*, 5 (2013) 6880.
27 Knyaz V A & Chibunichev A G, *Remote Sens Spatial Inform Sci*, 41 (2016) 515.